crude lactol which was immediately added to a vigorously stirring suspension[19] of pyridinium chlorochromate (200 mg) and neutral alumina (200 mg) in CH_2Cl_2 (4 mL). After 8 h, the mixture was diluted with Et_2O (20 mL) and filtered through a short bed of Florisil. The filtrate was washed with 5% $NaHCO_3$ solution and brine and evaporated to an oil: TLC, SiO_2, 1:1 Et_2O/hexane, $R_f \sim 0.32$; NMR 0.91 (3 H, d, $J \sim 7$ Hz), 0.95 (3 H, t, $J \sim 7$ Hz), 1.12 (9 H, s), 1.20 (3 H, d, $J \sim 7$ Hz), 1.20–2.60 (21 H, complex m), 4.12–4.40 (1 H, m), 4.56–4.92 (1 H, m), 5.18 (1 H, br s), 5.42 (1 H, br d, $J \sim 10$ Hz), 5.64 (1 H, ddd, $J \sim 2.5$, 4.5, 10 Hz), 7.30–7.50 (6 H, m), 7.50–7.75 (4 H, m). Desilylation using 48% hydrofluoric acid in acetonitrile (5 mL, 1:10) at 45 °C for 8 h, neutralization with saturated $NaHCO_3$ solution, extractive isolation, and chromatography (SiO_2, Et_2O, $R_f \sim 0.23$) afforded **3** (16 mg, 50%); mp 103–105 °C (benzene/hexane): $[\alpha]^{24}_D + 129°$ (*c* 1.3, $CHCl_3$), whose 360-MHz ^1H NMR spectrum was identical with that of natural material:[20] NMR 0.83 (3 H, d, $J \sim 7$ Hz), 0.89 (3 H, t, $J \sim 7$ Hz), 1.13 (3 H, d, $J \sim 7$ Hz), 1.30–2.60 (20 H, m), 2.56–2.76 (2 H, m), 4.20–4.42 (1 H, m), 4.42–4.80 (1 H, m), 5.16 (1 H, br s), 5.37 (1 H, br d, $J \sim 10$ Hz), 5.60 (1 H, ddd, $J \sim 2.5$, 4.5, 10 Hz); mass spectrum *m/e* (%) 393 ($M^+ + 1$, 2), 375 (2), 291 (14), 273 (61), 255 (9), 227 (4), 187 (34), 145 (100); high-resolution mass spectrum calcd for $C_{23}H_{36}O_5$ 392.2560, found 392.2554.

Acknowledgment. The authors are indebted to Dr. Akira Endo (Tokyo Noko University) for a generous give of (+)-compactin, Prof. Raymond Funk (University of Nebraska—Lincoln) for a sample and spectra of **11**, and Dr. Jean-Louis Gras (Marseille) for reference spectra.

Registry No. 3, 78366-44-6; **3** *t*-$BuPh_2Si$ derivative, 90344-22-2; **5**, 86031-03-0; **6**, 90344-09-5; **7**, 90344-10-8; **8**, 90344-11-9; **8** ethylene glycol ketal derivative, 90344-17-5; **9**, 90344-12-0; **9** keto-iodide derivative, 90344-18-6; **9** keto-sulfone derivative, 90367-63-8; **10**, 90344-13-1; **13**, 90344-14-2; **13** keto-sulfone derivative, 90344-19-7; **14**, 90367-62-7; **14** diastereomer, 90410-99-4; **14** ketone derivative, isomer 1, 90367-64-9; **14** ketone derivative, isomer 2, 90411-00-0; **14** (*S*)-(+)-2-methylbutyrate, 90344-20-0; **14** (*S*)-(+)-2-methylbutyrate demethyl derivative, 90344-21-1; dimethyl (*E,E*)-2,4-hexadienylmalonate, 75283-60-2; methyl (*E,E*)-4,6-octadienoate, 68823-50-7; (*E,E*)-octa-4,6-dien-1-ol, 80106-30-5; (*E,E*)-octa-4,6-dien-1-ol tosylate, 90344-15-3; sodium thiophenoxide, 930-69-8; (*E,E*)-1-(phenylthio)octa-4,6-diene, 90344-16-4; maleic anhydride, 108-31-6; 1,3-propanedithiol, 109-80-8.

Hydrogen Bonded Phosphate Esters. Synthesis and Structure of Catechol-Containing Salts of 2-Hydroxyphenyl Phenylphosphonate[1]

Charles A. Poutasse,[2] Roberta O. Day, and Robert R. Holmes*

Contribution from the Department of Chemistry, University of Massachusetts, Amherst, Massachusetts 01003. *Received September 8, 1983*

Abstract: The synthesis and X-ray structural analysis of the tetraphenylphosphonium salt of 2-hydroxyphenyl phenylphosphonate ($[(HOC_6H_4O)P(Ph)O_2][PPh_4]\cdot C_6H_4(OH)_2$ (**1**)) and the corresponding pyridinium salt ($[(HOC_6H_4O)P(Ph)O_2][C_5H_5NH]\cdot C_6H_4(OH)_2$ (**2**)) are reported. These substances form unique hydrogen bonded phosphonate ester systems which incorporate catechol molecules of crystallization. The hydrolysis reaction of the benzodioxaphosphole $[(C_6H_4O_2)_2PPh]$ with $KF\cdot 2H_2O$ and Ph_4PCl in acetonitrile gave the ester salt $[HOC_6H_4OP(Ph)O_2][PPh_4]$·catechol (**1**). By a similar method, the pyridinium salt was obtained ($[HOC_6H_4OP(Ph)O_2][C_5H_5NH]$·catechol (**2**)). Single-crystal X-ray analysis showed the phosphonate in **1** contained an intramolecular hydrogen bonded seven-membered ring. The phosphonates are linked by catechol molecules in a chain arrangement. In **2**, the pyridinium ion replaced the intramolecular ring in hydrogen bond formation. As a result, the structure shows dimeric phosphonate units linked together by catechol molecules in a doubly hydrogen bonded chain. **1** crystallizes in the monoclinic space group $P2_1/n$ with $a = 9.996$ (2) Å, $b = 26.858$ (7) Å, $c = 14.160$ (3) Å, $\beta = 109.57$ (1)°, and $Z = 4$. **2** crystallizes in the triclinic space group $P\bar{1}$ with $a = 9.074$ (2) Å, $b = 11.149$ (2) Å, $c = 11.786$ (2) Å, $\alpha = 70.26$ (2)°, $\beta = 87.54$ (2)°, $\gamma = 73.72$ (2)°, and $Z = 2$. A systematic classification of hydrogen bonding in phosphates is obtained regarding the number and types of interactions present in relation to the resultant structures. In addition, the O–X lengths increase with decreasing proton acidity in the hydrogen bonded phosphates, P=O···H—X (X = O, N). Little variation in the P=O bond lengths is apparent.

In modeling phosphoryl transfer enzyme reactions, it is necessary to incorporate hydrogen bonding and electrostatic interactions between the phosphorus-containing substrate and active site residues. The basis for estimating the magnitude of these terms and the conformational changes that are likely to occur as the reaction proceeds is usually limited. Our success in modeling ribonuclease action on uridylyl-(3′,5′)-adenosine[3] was directly dependent on the inclusion of structural parameters into the modeling program[4] based on earlier studies dealing with the structural determination of simpler tetra- and pentacoordinated phosphorus compounds.[5] The first step of action of this enzyme leading to a cyclic intermediate has limited phosphate–hydrogen bonding.[6] In staphylococcal nuclease, a system in which we are currently interested,[7,8] hydrogen bonding is more extensive.[9]

We wish to explore hydrogen bonding to model phosphate substrates that will allow an understanding of structural changes as the system becomes more complex. Examples from the lit-

(1) Presented at the International Conference on Phosphorus Chemistry, Nice, France, September 1983.
(2) This work represents a portion of the Ph.D. Thesis of C. A. Poutasse, University of Massachusetts, Amherst, MA.
(3) Holmes, R. R.; Deiters, J. A.; Gallucci, J. C. *J. Am. Chem. Soc.* **1978**, *100*, 7393.
(4) Deiters, J. A.; Gallucci, J. C.; Clark, T. E.; Holmes, R. R. *J. Am. Chem. Soc.* **1977**, *99*, 5461.
(5) Holmes, R. R. "Pentacoordinated Phosphorus"; American Chemical Society: Washington, DC, 1980; Vol. I, ACS Monogr. No. 175.
(6) Richards, F. M.; Wyckoff, H. W. "Atlas of Molecular Structures in Biology"; Phillips, D. C., Richards, F. M., Eds.; Clarendon Press: Oxford, 1973; Vol. 1.
(7) Deiters, J. A.; Gallucci, J. C.; Holmes, R. R. *J. Am. Chem. Soc.* **1982**, *104*, 5457.
(8) Deiters, J. A.; Holmes, R. R. *J. Am. Chem. Soc.* **1983**, *105*, 609.
(9) Cotton, F. A.; Hazen, E. E., Jr.; Legg, M. J. *Proc. Natl. Acad. Sci. U.S.A.* **1979**, *76*, 2551.

0002-7863/84/1506-3814$01.50/0

erature[10-15] reveal phosphorus structures containing a variety of hydrogen bonding arrangements in simple chains,[11-14] discrete dimeric units,[10,13,15] and columns or chains of dimeric units.[16] In some of these, the hydrogen bonding takes place between phosphate units, while in others, a cationic base portion is interposed between phosphates.[12]

We have prepared two unique hydrogen bonded phosphonate ester systems which incorporate catechol molecules that in one case isolate the phosphonate ester units from each other ($[(HOC_6H_4O)P(Ph)O_2][PPh_4]\cdot C_6H_4(OH)_2$ (**1**)) and in the other isolate dimeric phosphonates from each other ($[(HOC_6H_4O)P(Ph)O_2][C_5H_5NH]\cdot C_6H_4(OH)_2$ (**2**)). This paper reports their synthesis and X-ray structures. The formation of these hydrogen bonded networks is considered relative to other systems and shown to provide a systematic formulation of hydrogen bonding useful in understanding specific phosphate–substrate interactions.

Experimental Section

Preparation of Tetraphenylphosphonium 2-Hydroxyphenyl Phenylphosphonate·Catechol ($[(HOC_6H_4O)PO_2Ph][Ph_4P]\cdot C_6H_4(OH)_2$ (1)). 2-Phenyl-2,2′-spirobis(1,3,2-benzodioxaphosphole), prepared as detailed by Wieber and Hoos[17] (0.8292 g, 2.557 mmol), was dissolved in 50 mL of dry acetonitrile along with tetraphenylphosphonium chloride (0.9611 g, 2.564 mmol). Under nitrogen, an excess of potassium fluoride dihydrate (1.1497 g, 12.21 mmol) was added with stirring. The solution refluxed for 20 h, while the potassium fluoride crystals seemed to disappear and to be replaced by a white powder. The mixture was filtered to yield a clear, colorless solution. The volume was reduced to 10 mL by rotovaping, and 5 mL of ether was added. Cooling produced a white, crystalline solid which was filtered, recrystallized from an acetonitrile–ether solution (1:1), and dried under vacuum: weight 1.232 g (69% yield); mp 139–140 °C; ^{1}H NMR (CD_3CN–Me_2SO) δ 6.45–6.9 (m, 8 H), 7.15–7.4 (m, 3 H), 7.5–7.95 (m, 22 H). Anal. Calcd for $C_{42}H_{36}O_6P_2$: C, 72.20; H, 5.19; P, 8.87. Found: C, 72.31; H, 5.40; P, 8.69.

Preparation of Pyridinium 2-Hydroxyphenyl Phenylphosphonate·Catechol, ($[(HOC_6H_4O)PO_2Ph][C_5H_5NH]\cdot C_6H_4(OH)_2$ (2)). *o*-Phenylene phenylphosphonite, prepared according to Wieber and Hoos[17] (1.4233 g, 6.584 mmol), was dissolved in 30 mL of dry ether under nitrogen and cooled in an ice bath. Pyridine (0.5208 g, 6.585 mmol) was added with stirring. Catechol (0.7388 g, 6.709 mmol) was dissolved in 30 mL of dry ether and added dropwise. The solution was refluxed for 2 h and then cooled with no solid forming. The volume was reduced to 10 mL by evaporation, and cooling produced a tan solid. This was filtered out, washed with ether, and dried under vacuum. A second crop was obtained by further volume reduction: weight 1.487 g (51% yield); mp 125–126.5 °C; ^{1}H NMR (CD_3CN–Me_2SO) δ 6.45–6.85 (m, 8 H), 7.3–7.9 (br 6 H), 8.7 (s, 4 H). Anal. Calcd for $C_{23}H_{22}O_6NP$: C, 62.87; H, 5.05; N, 3.19; P, 7.05. Found: C, 63.00; H, 5.14; N, 3.16; P, 6.97.

Crystallography of 1 and 2. All X-ray crystallographic studies were done on an Enraf-Nonius CAD4 diffractometer with graphite monochromated molybdenum radiation ($\lambda_{K\alpha_1}$ = 0.70930 Å, $\lambda_{K\alpha_2}$ = 0.71359 Å) at an ambient temperature of 23 ± 2 °C. Details of the experimental and computational procedures have been described previously.[18]

Crystals for the X-ray determinations were grown by slow evaporation of a solution of each of the products dissolved in dry acetonitrile and mounted inside sealed, thin-walled, glass capillaries as a precaution against moisture sensitivity.

Crystal data for 1: $C_{36}H_{30}O_4P_2\cdot C_6H_6O_2$, colorless, 0.13 × 0.25 × 0.30 mm, uniquely determined monoclinic space group $P2_1/n$ (alternate setting of $P2_1/c$ [C_{2h}^5, No. 14][19a]), a = 9.996 (2) Å, b = 26.858 (7) Å, c = 14.160 (3) Å, β = 109.57 (1)°, Z = 4, and $\mu_{Mo\ K\alpha}$ = 0.175 mm^{-1}; 4115 independent reflections ($+h,+k,\pm l$) were measured by using the θ–2θ scan mode for $2° \le 2\theta_{Mo\ K\alpha} \le 43°$; no corrections were made for absorption.

The structure was solved by a combination of direct methods (MULTAN) and Fourier difference techniques and was refined by full-matrix least squares.[20] The 50 independent nonhydrogen atoms were refined anisotropically while the 3 hydroxyl hydrogen atoms (located on a difference Fourier) were refined isotropically. The 33 aromatic hydrogen atoms were included in the refinement as fixed isotropic scatterers (calculated coordinates updated as refinement converged so that the final C–H bond lengths were 0.98 Å). The final agreement factors[21] were R = 0.045 and R_w = 0.051 for the 2470 reflections having $I \ge 2\sigma_I$.

Crystal data for 2: $C_{17}H_{16}O_4NP\cdot C_6H_6O_2$, colorless, 0.19 × 0.21 × 0.30 mm, triclinic space group $P\bar{1}$ [C_i^1, No. 2],[19b] a = 9.074 (2) Å, b = 11.149 (2) Å, c = 11.786 (2) Å, α = 70.26 (2)°, β = 87.54 (2)°, γ = 73.72 (2)°, Z = 2, and $\mu_{Mo\ K\alpha}$ = 0.174 mm^{-1}; 3374 independent reflections ($+h,\pm k,\pm l$) were measured as for **1**.

The sructure was solved and refined as for **1** (31 non-hydrogen atoms anisotropic, 4 ΔF hydrogen atoms isotropic, 18 calculable C–H hydrogen atoms fixed isotropic) except that all hydrogen thermal parameters were fixed. The final agreement factors were R = 0.058 and R_w = 0.078 for the 2422 reflections having $I \ge 2\sigma_I$.

Results and Discussion

Synthesis. The reactions (eq 1 and 2) leading to the formation of the phenylphosphonates **1** and **2** involve a partial hydrolysis. In the case of **2**, an oxidation of the reactant phosphine occurs as well.

Scheme I

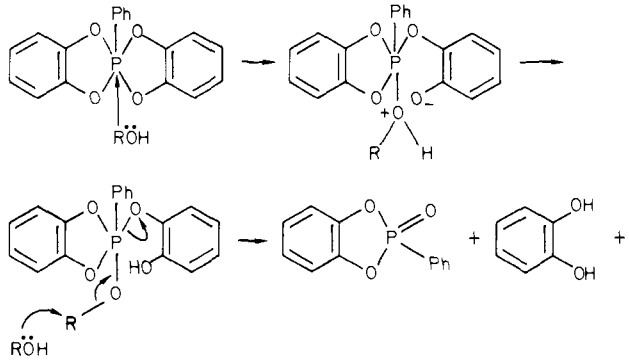

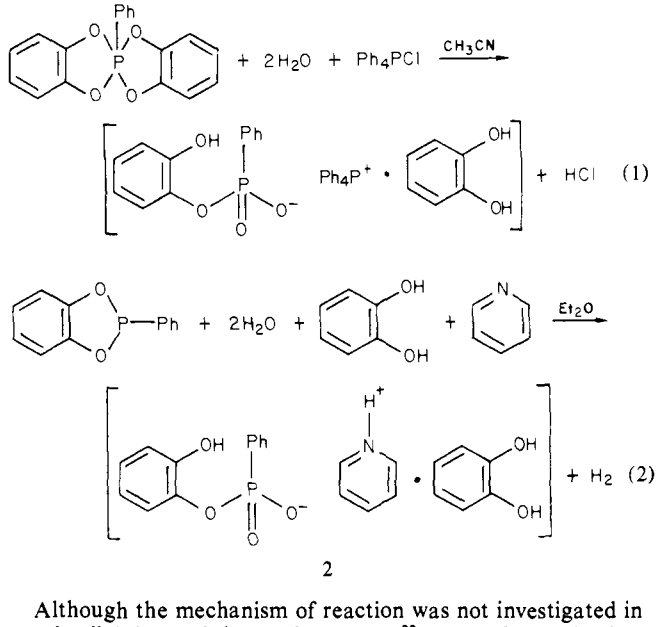

2

Although the mechanism of reaction was not investigated in any detail, it is noted that Cadogan et al.[22] proposed a mechanism

(10) Tkachev, V. V.; Atovmyan, L. O.; Kardanov, N. A.; Godovikov, N. N.; Kabachnik, M. I. *Zh. Strukt. Khim.* **1978**, *19*, 962.
(11) Antipin, M. Yu.; Struchkov, Yu. T.; Matrosov, E. I.; Bondarenko, N. A.; Tsvetkov, E. N.; Kabachnik, M. I. *Zh. Strukt. Khim.* **1981**, *22*, 100.
(12) Wieczorek, M. W.; Karolak-Wojciechowska, J.; Mikolajczyk, M.; Witczak, M. *Acta Crystallogr., Sect. B* **1978**, *B34*, 3138.
(13) du Plessis, M. P.; Modro, T. A.; Nassimbeni, L. R. *Acta Crystallogr., Sect. B* **1982**, *B38*, 1504.
(14) Sundaralingam, M.; Harmony, T. P.; Prusiner, P. *Acta Crystallogr., Sect. B* **1982**, *B38*, 1536.
(15) Varughese, K. I.; Lu, C. T.; Kartha, G. *J. Am. Chem. Soc.* **1982**, *104*, 3398.
(16) Brianso, M.-C.; Surcouf, E. *Acta. Crystallogr., Sect. B* **1978**, *B34*, 681.
(17) Wieber, M.; Hoos, W. R. *Monatsch. Chem.* **1970**, *101*, 776.
(18) Sau, A. C.; Day, R. O.; Holmes, R. R. *Inorg. Chem.* **1981**, *20*, 3076.
(19) (a) "International Tables for X-ray Crystallography"; Kynoch Press: Birmingham, England, 1969; Vol. I, p 99; (b) Reference 19a, p 75.
(20) The function minimized was $\sum w(|F_o| - |F_c|)^2$, where $w^{1/2} = 2F_oLp/\sigma_I$. Mean atomic scattering factors were taken from ref 19, Vol. IV, 1974, pp 72–98. Real and imaginery dispersion corrections for O and P were taken from the same source, pp 149–150.
(21) $R = \sum||F_o| - |F_c||/\sum|F_o|$ and $R_w = \{\sum w(|F_o| - |F_c|)^2/\sum w|F_o|^2\}^{1/2}$.

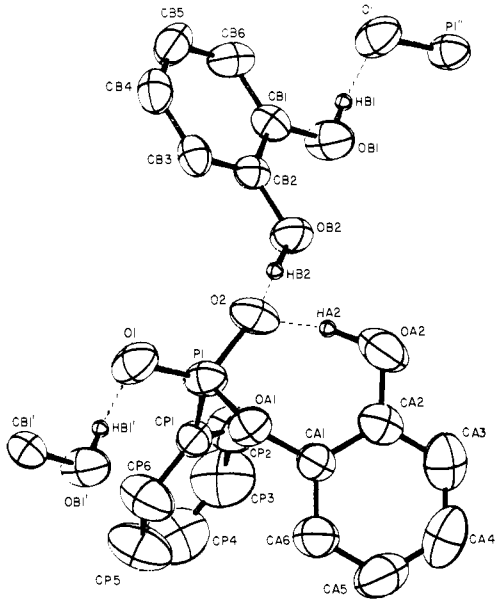

Figure 1. ORTEP plot of the anion and catechol moieties in $[(HOC_6H_4O)PO_2Ph][Ph_4P]\cdot C_6H_4(OH)_2$ (**1**) with thermal ellipsoids at the 50% probability level. Hydrogen bonds are shown as dashed lines. Primed and double-primed fragments are related by translations along *a* and are included to show the nature of the hydrogen bonded chains.

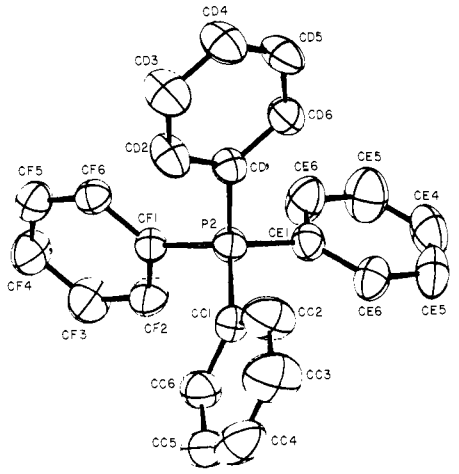

Figure 2. ORTEP plot of the cation in $[(HOC_6H_4O)PO_2Ph][Ph_4P]\cdot C_6H_4(OH)_2$ (**1**) with thermal ellipsoids at the 50% probability level.

for a reaction similar to that involved in the synthesis of **1**, starting with a nucleophilic attack on a five-coordinated spirophosphorane, Scheme I. The nucleophile is diphenylmethanol, instead of water, which would be the nucleophile in the reactions here. Although this mechanism is suggested for the formation of **1**, a critical assessment requires further work.

While the adaptation of Scheme I to the formation of **1** is clear, the steps by which **2** forms are highly uncertain.

Structure. The atom labeling scheme for **1** is given in the ORTEP plots of Figures 1 and 2. Refined atomic coordinates are given in Table I, and important bond lengths and angles are given in Table II. For **2**, the corresponding information is given in Figure 3 and in Tables III and IV. For both **1** and **2**, anisotropic thermal parameters, calculated hydrogen atom coordinates, and additional bond lengths and angles are provided as supplementary material.

Cocrystallization of the catechol moiety in both **1** and **2** is apparently caused by extensive hydrogen bonding interactions, but since the cation in **2** also participates in the hydrogen bonding, the two structures differ considerably.

In **1**, there is an intraanionic hydrogen bond between the hydroxyl hydrogen atom, HA2, and a phosphoryl oxygen atom, O2, resulting in the formation of a seven-membered ring (see Figure 1). The catechol moieties lie between translationally related anions forming infinite hydrogen bonded chains in which each of the catechol hydrogen atoms is hydrogen bonded to a different phosphonyl oxygen atom of the anions. The hydrogen bond lengths are HA2---O2 = 1.56 (9) Å, HB1---O1 = 1.71 (6) Å, and HB2---O2 = 1.59 (6) Å, as compared to the van der Waal's sum of 2.6 Å.[23]

Table I. Atomic Coordinates in Crystalline $[(HOC_6H_4O)PO_2Ph][Ph_4P]\cdot C_6H_4(OH)_2$ (**1**)[a]

atom type[b]	10^4x	10^4y	10^4z
P1	2973 (1)	5957 (1)	2827 (1)
P2	6899 (1)	3422 (1)	2394 (1)
O1	4149 (4)	6244 (1)	3534 (3)
O2	1497 (4)	6161 (1)	2535 (3)
OA1	3388 (3)	5922 (1)	1819 (2)
OA2	600 (5)	6138 (2)	531 (3)
OB1	−3304 (4)	6116 (1)	3326 (3)
OB2	−874 (4)	6081 (1)	2946 (3)
CA1	2682 (6)	5627 (2)	990 (4)
CA2	1345 (6)	5745 (2)	353 (4)
CA3	733 (7)	5464 (3)	−496 (4)
CA4	1474 (8)	5079 (3)	−717 (5)
CA5	2804 (8)	4957 (2)	−87 (5)
CA6	3415 (6)	5238 (2)	775 (4)
CB1	−2240 (5)	6433 (2)	3848 (4)
CB2	−975 (5)	6423 (2)	3630 (3)
CB3	101 (5)	6748 (2)	4116 (4)
CB4	−46 (6)	7086 (2)	4812 (4)
CB5	−1283 (6)	7090 (2)	5041 (4)
CB6	−2382 (6)	6763 (2)	4558 (4)
CP1	2981 (5)	5326 (2)	3225 (3)
CP2	1751 (6)	5076 (2)	3150 (5)
CP3	1796 (8)	4581 (3)	3450 (6)
CP4	3072 (10)	4340 (2)	3823 (6)
CP5	4270 (8)	4578 (3)	3877 (6)
CP6	4251 (6)	5072 (2)	3604 (5)
CC1	8482 (5)	3141 (2)	2302 (3)
CC2	9467 (6)	3448 (2)	2107 (5)
CC3	10689 (7)	3249 (3)	2018 (5)
CC4	10921 (7)	2744 (3)	2113 (4)
CC5	9955 (7)	2440 (2)	2287 (4)
CC6	8716 (6)	2632 (2)	2382 (4)
CD1	7364 (5)	4032 (2)	2906 (3)
CD2	8341 (5)	4078 (2)	3875 (4)
CD3	8648 (6)	4546 (2)	4300 (4)
CD4	8051 (6)	4964 (2)	3758 (4)
CD5	7168 (6)	4924 (2)	2802 (4)
CD6	6781 (6)	4456 (2)	2366 (4)
CE1	5555 (5)	3467 (2)	1185 (3)
CE2	5881 (6)	3468 (2)	310 (4)
CE3	4806 (7)	3522 (2)	−609 (4)
CE4	3436 (7)	3575 (2)	−652 (4)
CE5	3085 (6)	3572 (2)	207 (4)
CE6	4148 (6)	3517 (2)	1134 (4)
CF1	6175 (5)	3059 (2)	3175 (3)
CF2	5555 (6)	2602 (2)	2805 (4)
CF3	5002 (6)	2305 (2)	3377 (4)
CF4	5056 (6)	2460 (2)	4324 (4)
CF5	5642 (6)	2911 (2)	4682 (4)
CF6	6206 (5)	3218 (2)	4117 (3)
HA2	1000 (91)	6217 (31)	1370 (68)
HB1	−4198 (66)	6163 (22)	3450 (43)
HB2	97 (59)	6084 (20)	2813 (38)

[a] Numbers in parentheses are estimated standard deviations. [b] Atoms are labeled to agree with Figures 1 and 2.

(22) Cadogan, J. I. G.; Gosney, I.; Randles, D.; Yaslak, S. "Phosphorus Chemistry Proceedings of the 1981 International Conference"; Quin, L. D., Verkade, J. G., Eds., 1981; ACS Symp. Ser. No. 171, p. 41.

(23) Pauling, L. "The Nature of the Chemical Bond"; 3rd ed.; Cornell University Press: Ithaca, New York, 1960; p 260.

Table II. Selected Bond Lengths (Å), Bond Angles (deg), and Interatomic Distances for $[(HOC_6H_4O)PO_2Ph][Ph_4P]\cdot C_6H_4(OH)_2$ (**1**)[a]

type[b]	length	type	length
P1–O1	1.480 (4)	OA2–HA2	1.14 (9)
P1–O2	1.496 (4)	OB1–HB1	0.97 (6)
P1–OA1	1.618 (3)	OB2–HB2	1.05 (6)
P1–CP1	1.785 (5)	O2···HA2	1.56 (9)
OA1–CA1	1.396 (6)	O2···HB2	1.59 (6)
OA2–CA2	1.362 (6)	O1···HB1	1.71 (6)
OB1–CB1	1.369 (6)	O2, OA2	2.675 (5)
OB2–CB2	1.362 (5)	O1, OB1	2.681 (5)
		O2, OB2	2.632 (5)

type	angle	type	angle
O1–P1–O2	118.9 (2)	OA2–HA2···O2	164 (7)
O1–P1–CP1	111.2 (2)	HA2···O2–P1	105 (3)
O1–P1–OA1	104.3 (2)	HA2···O2–HB2	106 (4)
CP1–P1–O2	109.6 (2)	P1–O2···HB2	139 (2)
CP1–P1–OA1	104.3 (2)	P1–O1···HB1	117 (3)
O2–P1–OA1	107.3 (2)	O2···HB2–OB2	172 (5)
P1–OA1–CA1	124.6 (3)	HB2–OB2–CB2	115 (3)
OA1–CA1–CA6	117.6 (5)	OB2–CB2–CB1	117.3 (4)
OA1–CA1–CA2	121.7 (5)	OB2–CB2–CB3	123.5 (4)
CA1–CA2–OA2	121.9 (5)	CB2–CB1–OB1	117.6 (5)
CA3–CA2–OA2	118.4 (6)	CB6–CB1–OB1	122.8 (5)
CA2–OA2–HA2	108 (4)	CB1–OB1–HB1	115 (4)
		OB1–HB1···O1	174 (5)

[a] Numbers in parentheses are estimated standard deviations. [b] Atoms are labeled to agree with Figure 1.

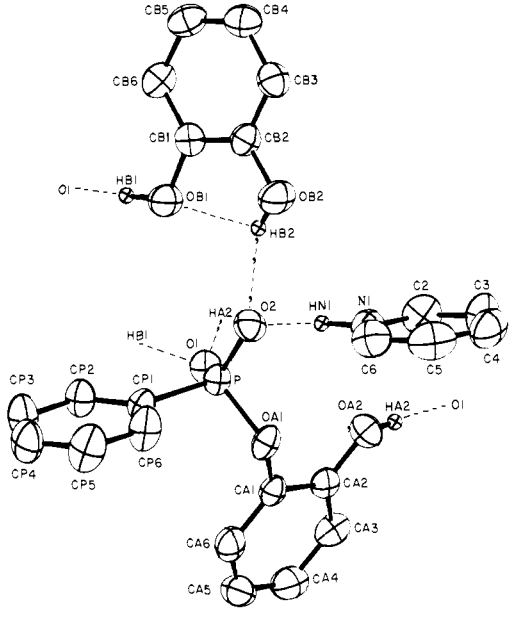

Figure 3. ORTEP plot of $[(HOC_6H_4O)PO_2Ph][C_5H_5NH]\cdot C_6H_4(OH)_2$ (**2**) with thermal ellipsoids at the 50% probability level. Hydrogen bonds are shown as dashed lines. Hydrogen bonds to symmetry-related atoms are shown schematically.

In **2** (Figure 4), inversion-related anions form dimeric hydrogen bonded units (HA2···O1 = 1.89 (6) Å). Via hydrogen bonding, an inversion-related pair of catechol molecules connects translationally related dimeric units (HB1···O1 = 1.69 (6) Å, HB2···O2 = 1.99 (6) Å) forming an infinite, doubly hydrogen bonded, zigzag chain to which the pyridinium ions are hydrogen bonded (HN1···O2 = 1.56 (6) Å).

It is seen that **2** utilizes both phosphoryl oxygen atoms in forming two hydrogen bonds each, while in **1** only one of the phosphoryl oxygen atoms is so utilized. In **2**, the replacement of the Ph_4P^+ cation by the pyridinium ion with its hydrogen bonding capability disallows the formation of an intramolecular hydrogen bonded ring system as in **1**. This releases the attached catechol moiety in **2** which logically leads to the dimerization of phosphonate ester units via the released catechol hydroxyl group. The latter group hydrogen bonds to the phosphoryl bond of the second phosphonate making up the dimer. This additional hydrogen bonding made possible in **2** accounts for the presence of two hydrogen bonds per phosphoryl group in this case.

Table III. Atomic Coordinates in Crystalline $[(HOC_6H_4O)PO_2Ph][C_5H_5NH]\cdot C_6H_4(OH)_2$ (**2**)[a]

atom type[b]	10^4x	10^4y	10^4z
P	1838 (1)	6496 (1)	6158 (1)
O1	2153 (3)	5237 (3)	5887 (3)
O2	1316 (3)	7787 (3)	5141 (3)
OA1	3393 (3)	6585 (3)	6714 (3)
OA2	5729 (3)	5863 (3)	5404 (3)
OB1	−1126 (4)	6909 (3)	3793 (3)
OB2	−14	9063 (3)	2923 (3)
CA1	4592 (5)	5432 (4)	7275 (4)
CA2	5790 (5)	5076 (4)	6566 (4)
CA3	6985 (5)	3928 (4)	7103 (4)
CA4	6988 (6)	3201 (5)	8299 (5)
CA5	5816 (6)	3587 (5)	9010 (4)
CA6	4602 (5)	4727 (5)	8484 (4)
CB1	−1680 (5)	7821 (4)	2676 (4)
CB2	−1109 (5)	8896 (4)	2264 (4)
CB3	−1597 (5)	9857 (4)	1130 (4)
CB4	−2705 (6)	9718 (5)	440 (4)
CB5	−3299 (5)	8668 (5)	854 (4)
CB6	−2798 (5)	7703 (4)	1982 (4)
CP1	529 (4)	6498 (4)	7345 (4)
CP2	−313 (5)	5605 (4)	7718 (4)
CP3	−1339 (6)	5662 (5)	8616 (5)
CP4	−1525 (6)	6626 (5)	9131 (5)
CP5	−706 (6)	7524 (6)	8765 (5)
CP6	314 (6)	7485 (5)	7864 (5)
N1	2835 (4)	9521 (4)	4225 (4)
C2	3928 (6)	9353 (5)	3442 (5)
C3	4694 (6)	10268 (6)	2979 (5)
C4	4338 (6)	11388 (5)	3299 (5)
C5	3222 (7)	11543 (5)	4105 (5)
C6	2465 (6)	10601 (5)	4547 (5)
HA2	6326 (70)	5662 (59)	4925 (56)
HB1	−1547 (67)	6103 (60)	3968 (51)
HB2	246 (73)	8421 (60)	3521 (58)
HN1	2238 (64)	8802 (55)	4528 (51)

[a] Numbers in parentheses are estimated standard deviations. [b] Atoms are labeled to agree with Figure 3.

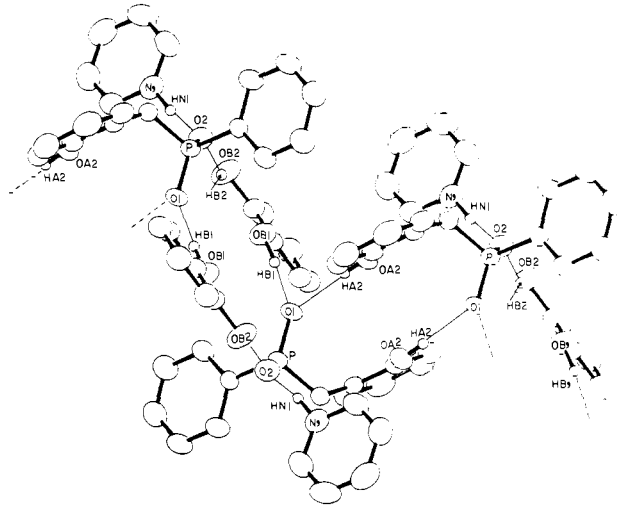

Figure 4. ORTEP plot showing the nature of the hydrogen bonded chains in $[(HOC_6H_4O)PO_2Ph][C_5H_5NH]\cdot C_6H_4(OH)_2$ (**2**). The two halves of the chain are related by inversion operations. Hydrogen bonds are shown as narrow solid lines. Extension of the chain, which zigzags along a, is indicated by the dashed lines.

Table IV. Selected Bond Lengths (Å), Bond Angles (deg), and Interatomic Distances (Å) for $[(HOC_6H_4O)PO_2Ph][C_5H_5NH]\cdot C_6H_4(OH)_2$ (2)[a]

type[b]	length	type	length
P-O1	1.493 (3)	OB2-HB2	0.80 (6)
P-O2	1.495 (3)	N1-HN1	1.05 (6)
P-OA1	1.623 (3)	O1---HA2	1.89 (6)
P-CP1	1.796 (4)	O1---HB1	1.69 (6)
OA1-CA1	1.406 (5)	O2---HN1	1.56 (6)
OA2-CA2	1.348 (5)	O2---HB2	1.99 (6)
OB1-CB1	1.373 (5)	O1, OA2	2.686 (4)
OB2-CB2	1.375 (5)	O1, OB1	2.711 (4)
OA2-HA2	0.81 (6)	O2, OB2	2.667 (4)
OB1-HB1	1.03 (6)	O2, N1	2.600 (5)
		OB1---HB2	2.30 (6)

type	angle	type	angle
O1-P-O2	118.5 (2)	CA2-OA2-HA2	123 (4)
O1-P-CP1	110.9 (2)	CB1-OB1-HB1	110 (3)
O1-P-OA1	109.9 (2)	CB2-OB2-HB2	109 (5)
CP1-P-O2	109.1 (1)	C2-N1-HN1	117 (3)
CP1-P-OA1	103.7 (2)	C6-N1-HN1	121 (3)
O2-P-OA1	103.4 (2)	OA2-HA2---O1	165 (6)
P-OA1-CA1	120.9 (2)	OB1-HB1---O1	174 (6)
OA1-CA1-CA6	120.9 (4)	OB2-HB2---O2	142 (6)
OA1-CA1-CA2	117.1 (4)	N1-HN1---O2	172 (5)
CA1-CA2-OA2	118.0 (4)	P-O2--HN1	128 (2)
CA3-CA2-OA2	123.9 (4)	P-O2---HB2	137 (2)
OB1-CB1-CB6	122.9 (4)	HN1---O2---HB2	85 (3)
OB1-CB1-CB2	117.1 (4)	P-O1---HA2	136 (2)
OB2-CB2-CB3	117.2 (4)	P-O1---HB1	145 (2)
OB2-CB2-CB1	122.1 (4)	HA2---P---HB1	79 (3)

[a] Numbers in parentheses are estimated standard deviations. [b] Atoms are labeled to agree with Figure 3.

Related Hydrogen Bonded Phosphates. All of the hydrogen bonded systems **3**–**7**[10-13] contain one hydrogen bond per phosphoryl group and give either chains or dimers. This is consistent with the availability of hydrogen bonding possibilities as outlined above for **1** and **2**.

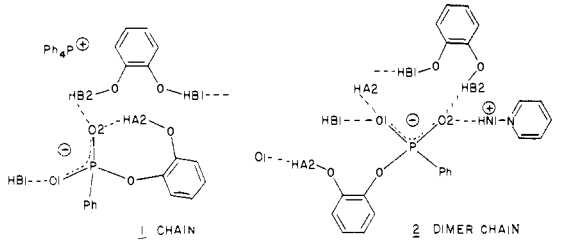

Our results on the catechol systems **1** and **2** dispel certain erroneous conclusions in some of the previous studies cited. The lack of formation of an intramolecular hydrogen bond in **4** is attributed[11] to steric effects in the seven-membered ring that would result. In our case, **1**, an intramolecular hydrogen bond forms giving an analogous seven-membered ring. The stability of a dimer formed by hydrogen bonding in **6** relative to a chain in **7** for two structures differing only in a *p*-nitro group is attributed[13] to a more linear hydrogen bond system in **6** (173°) relative to **7** (164°). In our work, we find the opposite, that the chain hydrogen bond in **1** with an angle of 174° is more linear than the dimer hydrogen bond in **2**, 165°.

It is apparent from this study that the hydrogen bonded structures examined may be placed on a systematic basis regarding the number and types of interactions in relation to their resultant structures. In the more complicated hydrogen bonded nucleotide formulations **8**[14] and **9**,[15] again a chain and a dimer formulation result. The authors[15] claim the dimer formulation is surprising. Relative to **8**, the result is expected. Similar to our observance that the pyridinium ion in **2** replaces the intramolecular hydrogen bonded ring in **1** and leads to the dimerization of **2**, the water

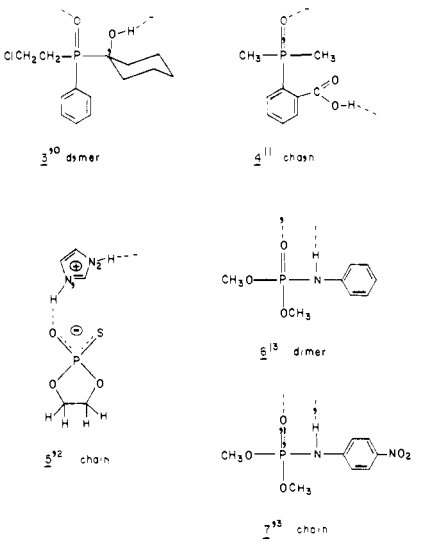

molcule present in **8** hydrogen bonds to the hydroxyl and amine functions that are involved in forming the dimeric units in **9**.

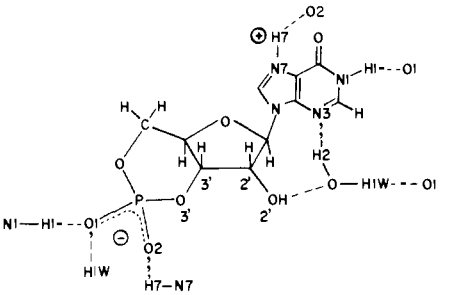

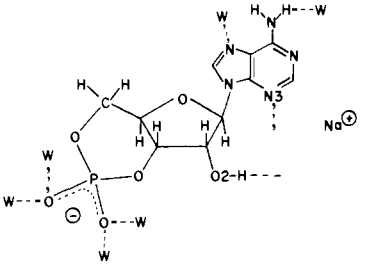

Hydrogen Bond Parameters. Table V summarizes hydrogen bond parameters for phosphoryl groups present in structures **1**–**9**. For these hydrogen bonds, there is little variation in the lengths of the P=O bonds as the hydrogen bond lengths vary, either for the O—O distances in the P=O---H—O bonds or the O—N distances in the P=O---H—N bonds. The hydrogen bond lengths, however, do show a general correlation with the acidity of the proton that is involved. For the P=O---H—O hydrogen bonds, the O—O lengths increase with decreasing proton acidity in the order CO_2H (**4**) > PhOH (**1**, **2**) > H_2O (**8**, **9**). The length changes from about 2.6 to 2.9 Å. In the related system, P=O---H—N, the O—N hydrogen bond lengths increase in the order N_7—H^+ (of inosine) ($\mathbf{8}_3$) > imidazolium protons

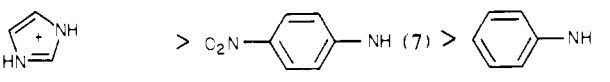

The lengths range from about 2.5 to 2.85 Å. Particularly for the P=O---H—O system, there is a decrease in hydrogen bond linearity as the O—O length increases, consistent with a drop off

Table V. Bond Parameters for Hydrogen Bonded Phosphoryl Groups

entry[a]	bond distances, Å[b]	A---B,[c] Å	A—H---B angle, deg	H bond type	no. of atoms per ring/ no. of H bonds	ref
$\mathbf{1}_1$	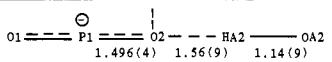	2.675 (5)	164 (7)	intramolecular ring	7/1	this work
$\mathbf{1}_2$	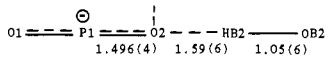	2.632 (5)	172 (5)	intermolecular chain		this work
$\mathbf{1}_3$	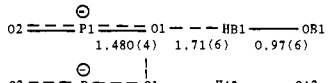	2.681 (5)	174 (5)	intermolecular chain		this work
$\mathbf{2}_1$	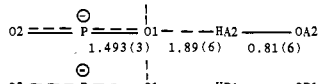	2.686 (4)	165 (6)	intermolecular dimer	14/2	this work
$\mathbf{2}_2$	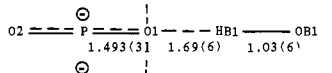	2.711 (4)	174 (6)	intermolecular dimer[d]	18/4	this work
$\mathbf{2}_3$	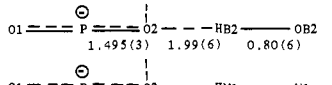	2.667 (4)	142 (6)	intermolecular dimer[d]	18/4	this work
$\mathbf{2}_4$	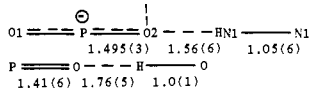	2.600 (5)	172 (5)	PyH^+		this work
3	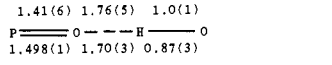		165.2 (8)	intermolecular dimer	10/2	10
4	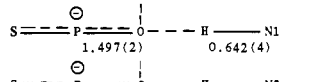	2.572 (1)	175 (3)	intermolecular chain		11
$\mathbf{5}_1$	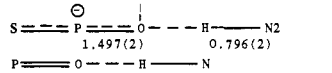	2.691	"linear"	intermolecular chain		12
$\mathbf{5}_2$	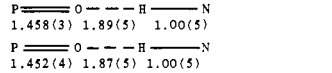	2.725	"linear"	intermolecular chain		12
6A[h]	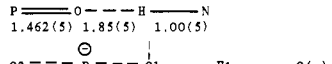	2.88 (1)	171.1 (9)	intermolecular dimer	8/2	13
6B	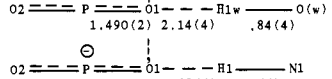	2.86 (1)	174.6 (9)	intermolecular dimer	8/2	13
7	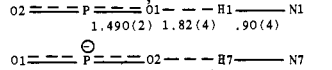	2.83 (5)	164.4 (9)	intermolecular chain		13
$\mathbf{8}_1$	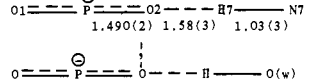	2.933 (4)	159 (4)	intermolecular polymer[e]	17/5	14
$\mathbf{8}_2$	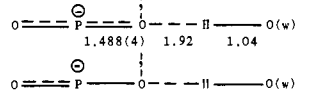	2.695 (3)	166 (4)	intermolecular polymer[e]	17/5	14
$\mathbf{8}_3$	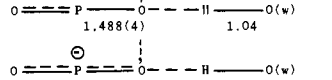	2.521 (3)	149 (3)	intermolecular polymer[f]	19/3	14
$\mathbf{9B}_1$[g,h]	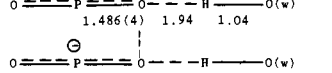	2.815	153	water molecule		15
$\mathbf{9B}_2$	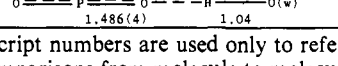	2.797		water molecule		15
$\mathbf{9B}_3$	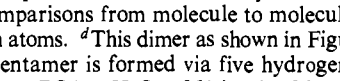	2.878	162	water molecule		15
$\mathbf{9B}_4$	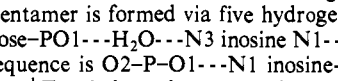	2.690		water molecule		15

[a] The subscript numbers are used only to refer to different entries for the same molecule. [b] The O---H hydrogen bond distances are not useful for comparisons from molecule to molecule because different treatments were used to fix the hydrogen atom positions. [c] A and B are non-hydrogen atoms. [d] This dimer as shown in Figure 4 contains two catechol molecules and two phosphate centers held together by four hydrogen bonds. [e] A pentamer is formed via five hydrogen bonds containing two water molecules and three CIMP zwitterions. The cyclic sequence is H_2O---ribose–PO1---H_2O---N3 inosine N1---PO1---. [f] A trimer is formed via three hydrogen bonds containing three CIMP zwitterions. The cyclic sequence is O2–P–O1---N1 inosine---O1P–ribose–inosine N7---. [g] For entry **9B** O(w) refers to one of the four molecules of crystallization. [h] Two independent molecules per unit cell exist for **6**[13] and **9**.[15] In **9**, the two molecules per asymmetric unit form a hydrogen bonded dimer via the adenosine N3 with the ribose O2 atom resulting in a 14-atom ring containing two hydrogen bonds. This differs for **6** where two independent centrosymmetrically related hydrogen bonded dimers form per unit cell.

in proton acidity. The range in angles is from 175° to about 160°.

In the light of these data, the lack of formation of a seven-membered ring by intramolecular hydrogen bonding in **4**[11] is probably associated with the attainment of hydrogen bond linearity in the strong hydrogen bond formed with the attached carboxyl group. The hydrogen bond angle in the observed chain conformation of **4** is 175°.[11] The intramolecular hydrogen bond in **1** resulting in a seven-membered ring has an angle of about 164°. If we sum the endo angles in the seven-membered ring of **1**, excluding the hydrogen bond angle, a value of 583.5° is obtained. Performing this same summation for **4** gives 587.3°. Hence, it seems unlikely that steric effect as stated[11] is the reason this ring does not form for **4**.

The phosphoryl group hydrogen bonds listed in Table V show their presence in rings that include the atom sizes 7–10, 14, 17, and 18. There is no discernible stability effect attributable to ring size as size varies over this set of relatively large rings. For smaller intramolecular hydrogen bonded ring systems, the order of stability observed in solution 8–7 > 6 > 5 has been reported.[24]

Acknowledgment. The support of this work by a grant from the National Institutes of Health (GM 21466) is gratefully acknowledged. We also express appreciation to the University of Massachusetts Computing Center for generous allocation of computer time.

Registry No. 1, 90220-04-5; **2**, 90220-06-7; 2-phenyl-2,2′-spirobis(1,3,2-benzodioxaphosphole), 21229-05-0; *o*-phenylene phenylphosphonite, 4759-37-9.

(24) Bondarenko, N. A. Thesis, Institute of Heteroorganic Compounds, Academy of Sciences, USSR, Moscow.

Supplementary Material Available: Listings of observed and calculated structure factor amplitudes for **1** and **2**; Table A, anisotropic thermal parameters for **1**; Table B, hydrogen atom parameters for **1**; Table C, additional bond lengths and angles for **1**; Table D, anisotropic thermal parameters for **2**; Table E, hydrogen atom parameters for **2**; and Table F, additional bond lengths and angles for **2** (27 pages). Ordering information is given on any current masthead page.

Mechanism of β-Lactam Ring Opening in Cephalosporins

Michael I. Page* and Philip Proctor

Contribution from the Department of Chemical Sciences, The Polytechnic, Huddersfield HD1 3DH, England. *Received July 19, 1983*

Abstract: There is a nonlinear dependence of the rate of aminolysis of some cephalosporins upon hydroxide ion concentration which is interpreted in terms of formation of a tetrahedral addition intermediate. At high concentrations of hydroxide ion the rate-limiting step is formation of the tetrahedral intermediate but at low concentrations it is the diffusion-controlled encounter of the intermediate and hydroxide ion. Rate constants for the formation and breakdown of the intermediate are reported. The equilibrium constants for formation of the intermediates are between 10^{-8} and 10^{-10} L mol^{-1}. Contrary to other suggestions nucleophilic attack on the β-lactam carbonyl carbon is not concerted with the expulsion of a leaving group at C3′. The rate of breakdown of the tetrahedral intermediates to products in the uncatalyzed aminolysis reaction is ca. 10^6 s^{-1} and not dependent upon whether or not a leaving group is expelled at C3′. Expulsion of a leaving group at C3′ does not significantly enhance the rate of β-lactam carbonyl carbon–nitrogen bond fission.

Cephalosporins **1** belong to the β-lactam class of antibiotics.[1] They differ from the penicillins by characteristically having a potential leaving group, eg., acetate or pyridine, at C-3′ which is expelled during the reaction of nucleophiles with the β-lactam (eq 1).[2] It has been suggested, on the basis of MO calculations,

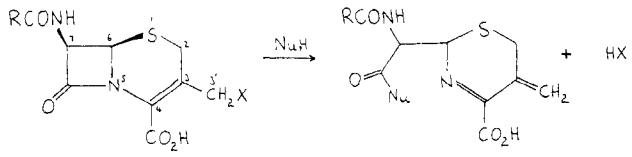

1 (1)

that nucleophilic attack on the β-lactam carbonyl is concerted with expulsion of the leaving group **2**.[3] Furthermore it has been

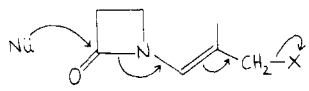

2

proposed that the biological activity of the cephalosporins is related to the ease of expulsion of the leaving group at C-3′.[4]

A reaction is concerted when it proceeds in one step because all "intermediate" species that would be formed are too unstable to exist. Substitution reactions at the carbonyl group proceed by mechanisms that are often enforced by the lifetime of the addition intermediates that may be formed during the reaction.[5,6] Although it has been suggested[7] that certain conformations of tetrahedral intermediates have lifetimes which are short compared with the times for intramolecular rotations (ca. 10^{-12} s),[8] a number of stable derivatives are known.[9] The reaction of amines with cephalosporins **1** (eq 1, Nu = RNH_2) requires proton removal from the attacking amine. Because of the relative time required for proton transfer and that for bond fission between heavy atoms this type of reaction may provide an experimental method for detecting and measuring the lifetime of intermediates.[10,11] The aminolysis of cephalosporins is also of interest because the primary allergic response is probably due to the formation of a protein conjugate resulting from the reaction of the ε-amino groups of lysine residues in proteins with the β-lactam.[12]

We present here evidence that the mechanism of the reaction of amines with cephalosporins is not concerted but a stepwise process involving the formation of a tetrahedral intermediate which then breaks down to products with little or no assistance from a potential leaving group at C3′.

Experimental Section

Materials. The cephalosporins were the generous gift of Glaxo Group Research (UK). The amines were purified by crystallization of the hydrochlorides or by distillation. Freshly boiled deionized water was used throughout.

Kinetics. The ionic strength was maintained at 1.0 M by the addition of potassium chloride unless otherwise stated. The reactions were initiated by the addition of 25 μL of aqueous 10^{-2} M cephalosporin to 2.5 cm^3 of the aqueous amine solution, preincubated at 30.0 ± 0.05 °C, with thorough mixing. The disappearance of the β-lactam was followed spectrophotometrically on a Gilford 240 spectrophotometer at 260 nm. The output from the spectrophotometer was fed into a Solarton data

(1) Page, M. I. *Acc. Chem. Res.* **1984**, *17*, 144.
(2) Hamilton-Miller, J. M. T.; Newton, G. G. F.; Abraham, E. P. *Biochem. J.* **1970**, *116*, 371. Hamilton-Miller, J. M. T.; Richards, E.; Abraham, E. P. *Ibid.* **1970**, *116*, 385. Bundgaard, H. *Arch. Pharm. Chemi., Sci. Ed.* **1975**, *3*, 94.
(3) Boyd, D. B.; Hermann, R. B.; Presti, D. E.; Marsh, M. M. *J. Med. Chem.* **1975**, *18*, 408. Boyd, D. B.; Lunn, W. H. W. *Ibid.* **1979**, *22*, 778.
(4) Boyd, D. B.; Herron, D. K.; Lunn, W. H. W.; Spitzer, W. A. *J. Am. Chem. Soc.* **1980**, *102*, 1812.
(5) Jencks, W. P. *Chem. Soc. Rev.* **1981**, *10*, 345.
(6) Jencks, W. P. *Acc. Chem. Res.* **1980**, *13*, 161.
(7) Deslongchamps, P. *Tetrahedraon* **1975**, *31*, 2463.
(8) Goldammer, E.; Zeidler, M. D. *Ber. Bunsenges. Phys. Chem.* **1969**, *73*, 4.
(9) Rogers, G. A.; Bruice, T. C. *J. Am. Chem. Soc.* **1973**, *95*, 4452. Hine, J.; Ricard, D.; Perz, R.; *J. Org. Chem.* **1973**, *38*, 110. Capon, B.; Ghosh, A. K. *J. Am. Chem. Soc.* **1981**, *103*, 1765. Guthrie, J. P. *Can. J. Chem.* **1976**, *56*, 202.
(10) Jencks, W. P. *Acc. Chem. Res.* **1976**, *9*, 425.
(11) Page, M. I.; Jencks, W. P. *J. Am. Chem. Soc.* **1972**, *94*, 8828.
(12) Assem, E. S. K.; Vickers, M. R. *Immunology* **1974**, *27*, 255. Mine, Y.; Mishida, M.; Goto, S.; Kuwahara, S. *J. Antibiot.* **1970**, 23, 195. Shibata, K.; Atsumi, Y.; Horiuchi, Y.; Mashimo, K., *Nature (London)* **1966**, *212*, 419.

0002-7863/84/1506-3820$01.50/0